

RESEARCH ARTICLE

The exported chaperone Hsp70-x supports virulence functions for *Plasmodium falciparum* blood stage parasites

Sarah C. Charnaud¹, Matthew W. A. Dixon^{2,3}, Catherine Q. Nie¹, Lia Chappell⁴, Paul R. Sanders¹, Thomas Nebi⁵, Eric Hanssen³, Matthew Berriman⁴, Jo-Anne Chan¹, Adam J. Blanch^{2,3}, James G. Beeson¹, Julian C. Rayner⁴, Jude M. Przyborski⁶, Leann Tilley^{2,3}, Brendan S. Crabb^{1,2,7}, Paul R. Gilson^{1,7*}

1 Burnet Institute, Melbourne, Victoria, Australia, **2** Department of Biochemistry and Molecular Biology, The University of Melbourne, Melbourne, Victoria, Australia, **3** Bio21 Molecular Science and Biotechnology Institute, The University of Melbourne, Melbourne, Victoria, Australia, **4** Wellcome Trust Sanger Institute, Wellcome Genome Campus, Hinxton, Cambridgeshire, United Kingdom, **5** Walter & Eliza Hall Institute, Melbourne, Victoria, Australia, **6** Parasitology, FB Biology, Philips University Marburg, Marburg, Germany, **7** Monash University, Melbourne, Victoria, Australia

* gilson@burnet.edu.au



OPEN ACCESS

Citation: Charnaud SC, Dixon MWA, Nie CQ, Chappell L, Sanders PR, Nebi T, et al. (2017) The exported chaperone Hsp70-x supports virulence functions for *Plasmodium falciparum* blood stage parasites. PLoS ONE 12(7): e0181656. <https://doi.org/10.1371/journal.pone.0181656>

Editor: Tobias Spielmann, Bernhard Nocht Institute for Tropical Medicine, GERMANY

Received: March 27, 2017

Accepted: July 5, 2017

Published: July 21, 2017

Copyright: © 2017 Charnaud et al. This is an open access article distributed under the terms of the [Creative Commons Attribution License](https://creativecommons.org/licenses/by/4.0/), which permits unrestricted use, distribution, and reproduction in any medium, provided the original author and source are credited.

Data Availability Statement: All relevant data are within the paper and its Supporting Information files.

Funding: The authors would like to thank National Health and Medical Research Council (grant numbers 1092789 & 1078065), OzEMaR Researcher Exchange funding and Victorian Operational Infrastructure Support Program received by the Burnet Institute.

Competing interests: The authors have declared that no competing interests exist.

Abstract

Malaria is caused by five different *Plasmodium* spp. in humans each of which modifies the host erythrocyte to survive and replicate. The two main causes of malaria, *P. falciparum* and *P. vivax*, differ in their ability to cause severe disease, mainly due to differences in the cytoadhesion of infected erythrocytes (IE) in the microvasculature. Cytoadhesion of *P. falciparum* in the brain leads to a large number of deaths each year and is a consequence of exported parasite proteins, some of which modify the erythrocyte cytoskeleton while others such as PfEMP1 project onto the erythrocyte surface where they bind to endothelial cells. Here we investigate the effects of knocking out an exported Hsp70-type chaperone termed Hsp70-x that is present in *P. falciparum* but not *P. vivax*. Although the growth of $\Delta hsp70-x$ parasites was unaffected, the export of PfEMP1 cytoadherence proteins was delayed and $\Delta hsp70-x$ IE had reduced adhesion. The $\Delta hsp70-x$ IE were also more rigid than wild-type controls indicating changes in the way the parasites modified their host erythrocyte. To investigate the cause of this, transcriptional and translational changes in exported and chaperone proteins were monitored and some changes were observed. We propose that PfHsp70-x is not essential for survival *in vitro*, but may be required for the efficient export and functioning of some *P. falciparum* exported proteins.

Introduction

Nearly half of the world's population (3.2 of 7.1 billion) are at risk from contracting malaria, caused by the *Plasmodium* genus of intracellular parasites, which can cause severe life threatening disease and debilitating illness [1]. *Plasmodium* parasites amplify in the erythrocytes of their host animals, and to do so the parasites must remodel their host cells in order to import

plasma nutrients and evade the immune system. The most pathogenic *Plasmodium* species to humans is *Plasmodium falciparum* (*Pf*), which can cause severe morbidity and mortality. Many of the severe consequences in *Pf* infections are due to expression of an erythrocyte surface exposed exported protein, erythrocyte membrane protein 1 (*PfEMP1*). In a process known as cytoadherence, *PfEMP1* allows the infected erythrocytes (IE) to bind endothelial cells and avoid splenic clearance [2]. Cytoadherence can however occlude the microvasculature and cause severe pathogenesis, which in the brain can result in coma and death, and in the placenta of pregnant women can lead to fetal growth restriction and low birth weight, or pre-term birth [2–5].

In order to remodel their host cells *Pf* parasites export effector proteins into the erythrocyte cytoplasm and plasma membrane [5, 6]. These proteins must first traverse the parasite's plasma membrane into the parasitophorous vacuole (PV) space and then across the enveloping PV membrane (PVM). Proteins cross the PVM in an unfolded state [7] via a proteinaceous pore termed PTEX [8]. Most proteins destined for export via PTEX contain a pentameric PEXEL motif, although there are also many PEXEL-negative exported proteins (PNEPs) [8–12]. There are five core components of PTEX including HSP101, a Hsp100 chaperone that when functionally ablated causes rapid parasite death [13]. Hsp100 chaperones typically interact with other chaperone components, including Hsp70/Hsp40 pairs that can unfold and refold complex proteins [14, 15]. We recently identified a novel Hsp70, Hsp70-x, that is secreted into the PV where it can interact with PTEX, as well as being exported into the host erythrocyte [16–18].

Hsp70-x is specific to the *Laverania* sub-genus of *Plasmodium*, which includes *P. falciparum* and multiple related species that infect great apes [18]. Hsp70-x is absent from other *Plasmodium* species including *P. vivax*, the other major cause of human malaria. Functions common to *Laverania* species are the ability to invade both mature and immature erythrocytes known as reticulocytes [19], a large exportome of hundreds of PEXEL proteins [20], and an ability to strongly cytoadhere via surface virulence factors such as *PfEMP1* [21, 22]. In contrast, *P. vivax* only invades reticulocytes, exports fewer PEXEL proteins, and does not cytoadhere to the same extent resulting in reduced virulence [23–25]. We hypothesized that the presence of Hsp70-x in *P. falciparum* and *P. reichenowi* could be a contributing factor to one or all of these *Laverania* specific features.

Here we report on the successful genetic deletion of *hsp70-x* in *P. falciparum* resulting in no effect on growth or stress response *in vitro*. The Δ Hsp70-x parasites however have reduced virulence characteristics in *in vitro* assays, and the IE are less cytoadherent under flow conditions and are more rigid which might reduce their fitness *in vivo*. The parasites could have responded to genetic ablation of Hsp70-x by increasing the transcription and translation of some chaperones and exported proteins.

Materials and methods

Plasmid construction

To make a functional knockout of *hsp70-x* two flanking regions of ~1kb (Flank 1 and Flank 2) were cloned from the genomic DNA of the *P. falciparum* strain, 3D7. Flank 1 was amplified using primers TACATACCGCGGGTAACAATGCAGAAGAATCAGAGGTTGCA and TTTCAACTAGTATTAAAGTATTACGGAATTGATCCAT, and Flank 2 using primers CCAAGTCCATGGAATTGTTTAGTTGGTGGTTCA and CTTTATCCTAGGAATTACGACCTCTTAAGTTGGTTGCCT, with restriction sites underlined. The flanks were cloned into plasmid pCC1 either side of the DHFR cassette and double homologous recombination was driven by cytosine deaminase. Knockout was confirmed by PCR with primer pairs A/A' for *hsp70x* GCAAGAAACACCTAGA

AAATTACTG and GGAAACAATCCAAATGTTGTTGC, B/B' for cytosine deaminase ACACAGTAGTATCTGTCACCAAAGTCA and GTGACAGGGGGAATGGCAAGC, C/C' for *hsp70-x* 5' UTR TGCAACAACAACAGTACATACAGCAAGT and *hDHFR* ACGATGCAGTTTAGCGAACCATGC and D/D' for *hDHFR* CTGATGTCCAGGAGGAGAAAGGCAT and *hsp70x* 3' UTR TGGTTTAATT TACTTCTTCAACGGTTGGTCCA

P. falciparum culture and transfection

Parasites were grown as per a modified version of Trager and Jensen [26]. Briefly, parasites were grown in complete RPMI-1640-HEPES media (Sigma) supplemented with 0.25% AlbumaxII (Gibco) and 5% heat inactivated pooled human sera (Australian Red Cross Blood Service). Red blood cells (Australian Red Cross Blood Service) were transfected with 150 µg of plasmid DNA and trophozoites added. Single homologous recombination was driven with 6 cycles with 2.5nM WR99210. Parasites were successfully recovered and subjected to negative selection with 5-fluorocytosine [27] on alternate days for 5 days followed by continuous culture. Recovered parasites were cloned by limiting dilution.

Growth assays

Malstat assay to measure lactate dehydrogenase (LDH) correlates with parasitaemia and was performed as described previously [28]. Parasitaemia was adjusted to 0.2% parasitaemia in 2% haematocrit and seeded in triplicate and samples stored at -80°C. Assays were performed at the trophozoite stage in the absence of drug selection as described previously and absorbance measured at 630nm on Multiskan GO (Thermo Scientific).

Flow cytometry

iRBC at 0.04% haematocrit were washed once in 0.1% casein in PBS, and centrifuged at 2000g for two min. Cells were resuspended in 10 µg/mL ethidium bromide (Invitrogen) in 0.1% casein in PBS and incubated in the dark at room temperature for 20–40 minutes. Cells were washed and resuspended in PBS. Samples were analysed on a FACSCanto II. Labelling of IEs by antibodies present in serum from malaria-exposed pregnant women, to evaluate *PfEMP1* surface expression was performed as described previously [12]. Serum samples were obtained from pregnant women resident in a malaria-endemic region of Papua New Guinea and were previously tested to identify samples with antibody reactivity to the surface of CS2 IEs [29, 30]. Ethics approval was obtained from the Medical Research Advisory Committee, PNG, and the Human Research and Ethics Committee of Alfred Health, Australia. All subjects gave written informed consent.

Immunofluorescence assay (IFA)

IFAs were performed as described previously [12]. Briefly, the IFAs were performed on dried blood smears fixed for 5 minutes with cold 100% methanol. After drying the slides were blocked in 3% BSA. Primary antibodies were added at 1:500 of serum in 3% BSA. Secondary antibodies (AlexaFluor 488, 568 or 594) were added at 1:2000. Imaging was performed on a Zeiss Axio Observer ZV1 and analysed with Fiji v1.4. Measurement of mean fluorescence intensity was performed using Fiji by manually selecting the area outside the PVM marker EXP2, and within the erythrocyte boundary by DIC/Bright field.

Western blot analysis

Mixed ring and trophozoite stage parasites were passed through a magnetized column (Miltenyi) to separate trophozoites from rings. Whole trophozoite infected erythrocytes were resuspended in about 30 pellet volumes of SDS sample buffer and fractionated on 4–12% gels (Life Technologies) by SDS PAGE. The ring samples were lysed in 0.09% saponin, and washed in PBS to remove haemoglobin. The ring pellet was similarly prepared for SDS-PAGE. After transfer to nitrocellulose membrane the blots were probed with rabbit serum for KAHRP and SBP1 (kind gifts from Alan Cowman and Brian Cooke) at 1/500 in 1% casein. Rabbit serum for Hsp70-1 was produced by the Walter & Eliza Hall Institute Monoclonal facility and was similarly used at 1/1000. Mouse monoclonals for RESA 18.2 (a kind gift from Robin Anders) and EXP2 were used at 3 µg/mL. Secondary antibodies labeled with 700 and 800 nm fluorescent dyes were used at 1/5000 and detected with an Odyssey FC scanner (Li-Cor). Densitometry was performed using the Odyssey Image Studio software.

Cytoadhesion and cell rigidity assays

Cytoadhesion under flow conditions was performed as described previously [31], using a flow chamber coated with chondroitin sulfate A (CSA) at 100 µg/mL in PBS and imaged on a Delta-Vision microscope. Static flow was analysed with CSA bound to plastic dishes at 40 µg/mL. Cell deformability using artificial spleen model was performed as described previously [32]. Cells were synchronized by heparin and sorbitol to within a four hour window.

Scanning electron microscopy (SEM)

Cells were synchronized by heparin and sorbitol, then magnet purified to >90% iRBC at trophozoite stage and fixed in PBS with 1% glutaraldehyde, and stored at 4°C until needed. IE were washed in PBS with 3 centrifugation cycles (2 min at 300g) before being deposited onto coverslips coated with poly-L-lysine. Cells were dehydrated in a series of ethanol and water baths at 0, 20, 50, 70, 80, 90, 95, and 100% (x3) ethanol for 5 min each. Coverslips were coated with approximately 2 nm of Au prior to imaging in a FEI Teneo microscope operating at 2 kV with backscatter detection, using a working distance of 5 mm.

RNA-seq

Parasites were synchronized with sorbitol and heparin, and total RNA was prepared from different staged samples as per [33]. A Bioanalyzer Nano chip (Agilent) was used to QC and quantify total RNA. A modified RNA-seq protocol (“DAFT-seq”, [34]) was used to account for the extreme AT-content of the *P. falciparum* transcriptome. Briefly, polyA+ RNA (mRNA) was selected using magnetic oligo-d(T) beads (E7490, NEB). Reverse transcription using Superscript II (Life) was primed using oligo d(T) primers, then second strand cDNA synthesis included dUTP. The resulting cDNA was fragmented using a Covaris AFA sonicator (20% duty cycle; intensity 5; 200 cycles per burst for 30 s). A “with-bead” protocol was used for dA-tailing, end repair and adapter ligation (NEB) using “PCR-free” barcoded sequencing adaptors (similar to [35]). After 2 rounds of SPRI cleanup the libraries were eluted in EB buffer and USER enzyme mix (NEB) was used to digest the second strand cDNA, generating directional libraries. Samples were sent for sequencing without amplification where possible. For lower input samples (10–12 hours post invasion (hpi) and 20–24 hpi) libraries were amplified by 16 cycles of PCR with KAPA HIFI polymerase [36]. The libraries were quantified by qPCR and sequenced on an Illumina HiSeq2000. Data was analysed at the Wellcome Trust Sanger Institute, UK. Reference *Plasmodium* genomes for 3D7 and IT were downloaded from GeneDB

[37]. Reads were mapped with TopHat [38]. Differential expression was analysed using DESeq [39]. RNA-seq data was visualized in Artemis [40].

Stable-isotope labeling and chromatography mass spectrometry detection (SILAC)

SILAC labelling of blood-stage parasites was performed as previously outlined [41]. Briefly, parasites were grown for three cycles in heavy or light isoleucine media, and synchronized with sorbitol. Age-matched 20–28 hpi trophozoites were magnet purified and mixed in equal ratios. Equinatoxin in PBS was used to lyse the RBC membrane [42] and supernatant was collected. Haemoglobin was removed using Ni⁺ NTA resin (Sigma) prior to mass spectrometry performed exactly as described previously [16].

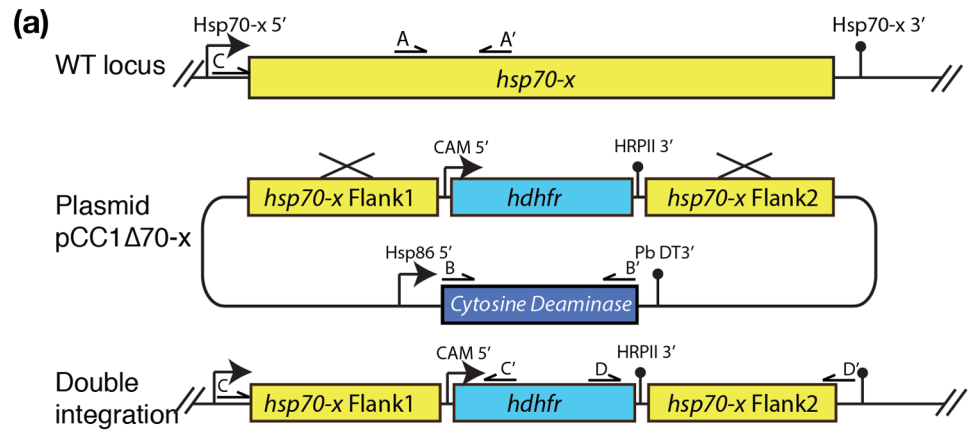
Results

Hsp70-x is not essential to survival

The *P. falciparum* line CS2 was used as the parental line for *hsp70-x* deletion as it expresses the stable and well characterized *PfEMP1* variant, VAR2CSA [5, 43]. To determine whether *P. falciparum* requires Hsp70-x to survive in mature erythrocytes or to export and functionalize its large exportome we attempted to delete the *hsp70-x* gene. A double homologous recombination method was used to replace *hsp70-x* with a human dihydrofolate reductase gene (*hdhfr*) cassette that conferred resistance to the antifolate WR99210 (Fig 1a). After multiple attempts, viable parasites were eventually recovered after six cycles of selection with WR99210 and negative selection cycles with 5-fluorocytosine to remove non-integrated plasmids. Anecdotally this indicated to us that deletion of *hsp70-x* was difficult to achieve.

Three clonal Δ Hsp70-x lines (A7, B10, G1) were established by limiting dilution, and the double recombination and gene replacement was confirmed by PCR (Fig 1b). To verify that *hsp70-x* had been ablated, western blot analysis was performed using antibodies specific to Hsp70-x (Fig 1c) [18]. All three clones no longer produced Hsp70-x with expression of the closely related cytoplasmic Hsp70-1 protein serving as a loading control. Subsequent experiments were performed on at least two of the three clones, and if no difference was observed between clones the combined data are reported.

The ability to isolate Δ Hsp70-x parasites indicated that Hsp70-x was not essential for survival *in vitro*. Growth rate as measured by the fold amplification of the parasites per cell cycle was measured and indicated that the mean fold increase in Δ Hsp-70x was not statistically significant to the parental CS2 line (Δ Hsp70-x 5.23(3.90–7.46) vs CS2 5.72(3.57–8.91) median (IQR)) (Fig 2a). To further confirm this, the number of merozoites per schizont was counted in each line, as well as the cell cycle length. Merozoite counts revealed no significant difference with each schizont containing a mean of ~11 merozoites (Fig 2b). Microscopy of Giemsa stained IE indicated that Δ Hsp70-x appeared similar to CS2 with no obvious abnormalities (Fig 2c). To more accurately quantify changes in maturation through the cell cycle, the DNA content of parasites stained with ethidium bromide was measured by flow cytometry (Fig 2d). This indicated that most parasites had the same DNA content at each timepoint and were maturing at the same rate. There were slightly more younger parasites in Δ Hsp70-x than CS2 represented by the 'tail' on the left in the 26–28 and 32–34 hpi samples. This is likely indicative of Δ Hsp70-x being less well synchronized rather than a slower cell cycle, which would be expected to reduce the overall growth rate and this was not observed.



PCR	1	2	3	4
Primers	A/A'	B/B'	C/C'	D/D'
Integrated	0	0	2.0kb	1.6kb
WT	0.4kb	0	0	0
Plasmid	0	1.1kb	0	0

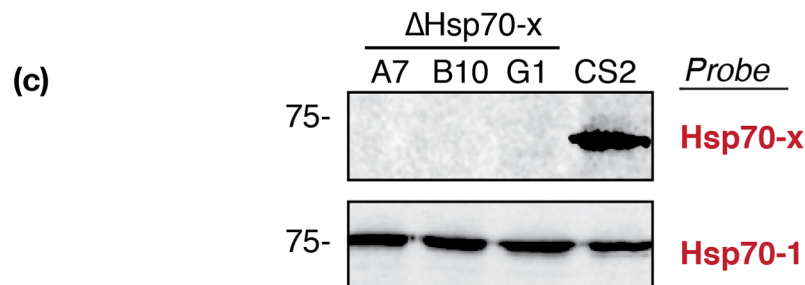
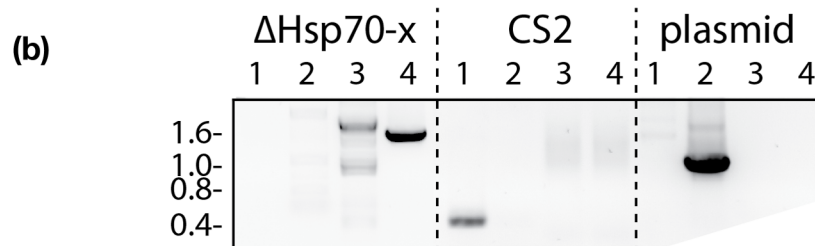


Fig 1. *hsp70-x* can be knocked out and is not essential for parasite survival. (a) Diagram of plasmid construct indicating double homologous recombination event to replace *hsp70-x* with a *dhfr* drug resistance cassette. Negative selection pressure to remove parasites carrying non-integrated plasmid is provided by the cytosine deaminase. The binding sites of PCR primers used to confirm gene replacement are indicated. (b) (Top) Table of PCR primer combinations and expected DNA product sizes resulting from amplification the native *hsp70-x* locus, the *dhfr* replacement locus and plasmid construct are shown. (Bottom) Agarose gel of PCR products from one $\Delta hsp70-x$ clone, the parental (CS2) parasites and plasmid only controls indicate the *hsp70-x* gene has been deleted by double cross over integration. (c) Western blot probed with rabbit anti-Hsp70-x confirms three separate $\Delta Hsp70-x$ clones no longer express Hsp70-x, but retain the closely related cytoplasmic Hsp70-1.

<https://doi.org/10.1371/journal.pone.0181656.g001>

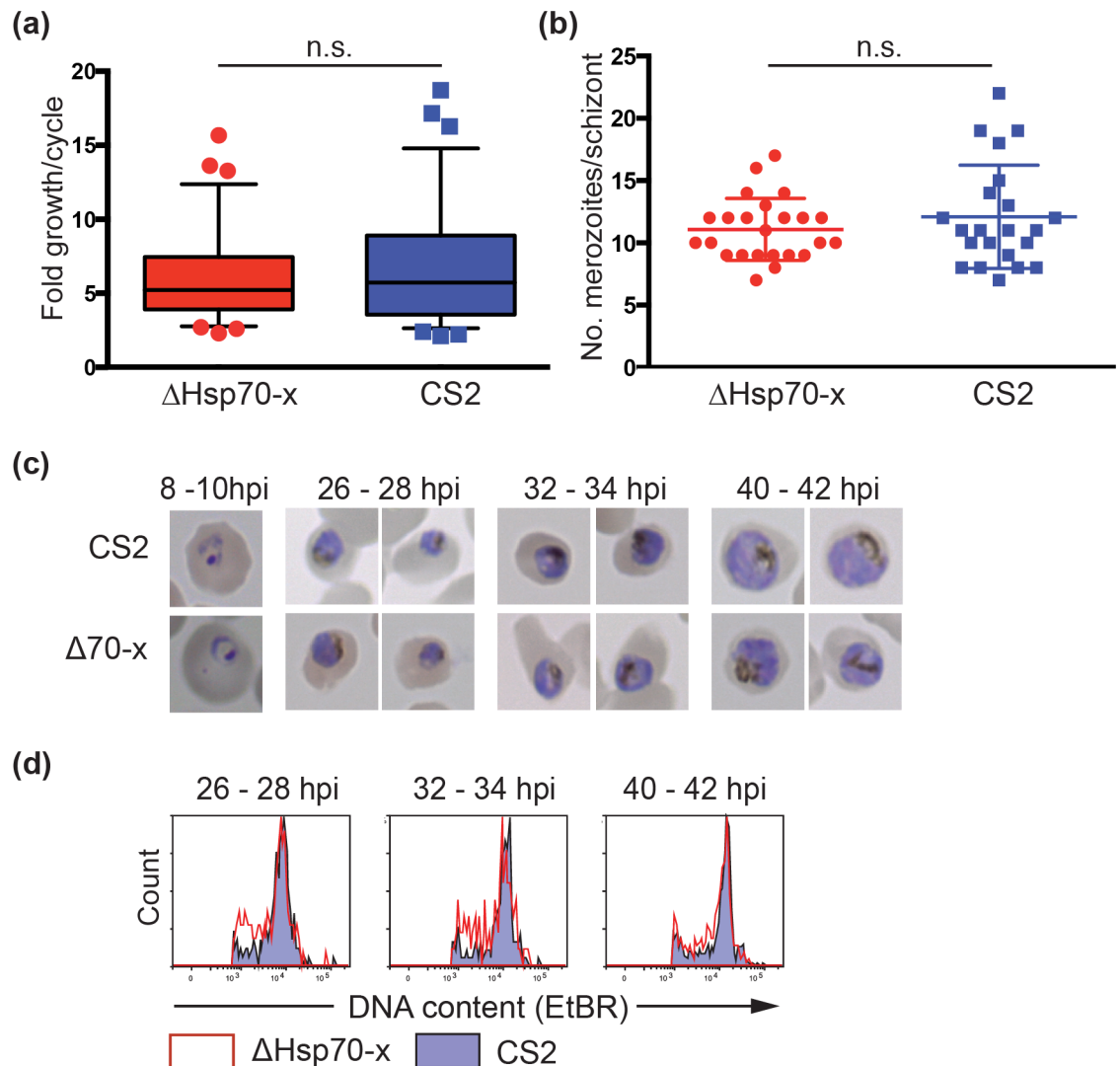


Fig 2. Deletion of *hsp70-x* does not affect parasite growth in the blood stage cell cycle. (a) Measurement of the fold increase cell proliferation per blood stage cycle of Δ Hsp70-x and CS2 parasites as assessed by parasite lactate dehydrogenase (LDH) activity indicates the growth of Δ Hsp70-x parasites was not significantly (n.s.) slower than CS2. Mann-Whitney $p = 0.7$, $n = 36$. (b) Light microscopy counts of the mean number of merozoites per schizont in Δ Hsp70-x and CS2 parasite lines indicated there was no significant difference. (c) Light microscopy images of four hour synchronized Giemsa stained parasites indicating both lines were morphologically similar. (d) Measurement of the DNA content of ethidium bromide (EtBR) stained Δ Hsp70-x and CS2 IE by flow cytometry indicates similar DNA content in the majority of cells at each time point. Parasites were synchronized to a four-hour window and the red trace indicates Δ Hsp70-x DNA content compared to CS2 in purple.

<https://doi.org/10.1371/journal.pone.0181656.g002>

Δ hsp70-x parasites are equally as susceptible to most stressors as CS2

Since Hsp70s are important for helping cells cope with heat and other stresses we subjected the Δ Hsp70-x parasites to a range of extreme conditions to determine if they were more vulnerable. Ring stage parasites were first heat shocked between 37°C and 42°C for six hours and then allowed to recover for 1.5 cell cycles (~72 h). Lactate dehydrogenase (LDH) activity was measured as a surrogate for parasite growth and indicated that Δ Hsp70-x growth was not reduced relative to CS2 (Fig 3a). Next parasite growth in an atmosphere containing standard parasite culture gas (5% CO₂, 94% N₂ and 1% O₂) or air containing 20% O₂ and 5% CO₂ was

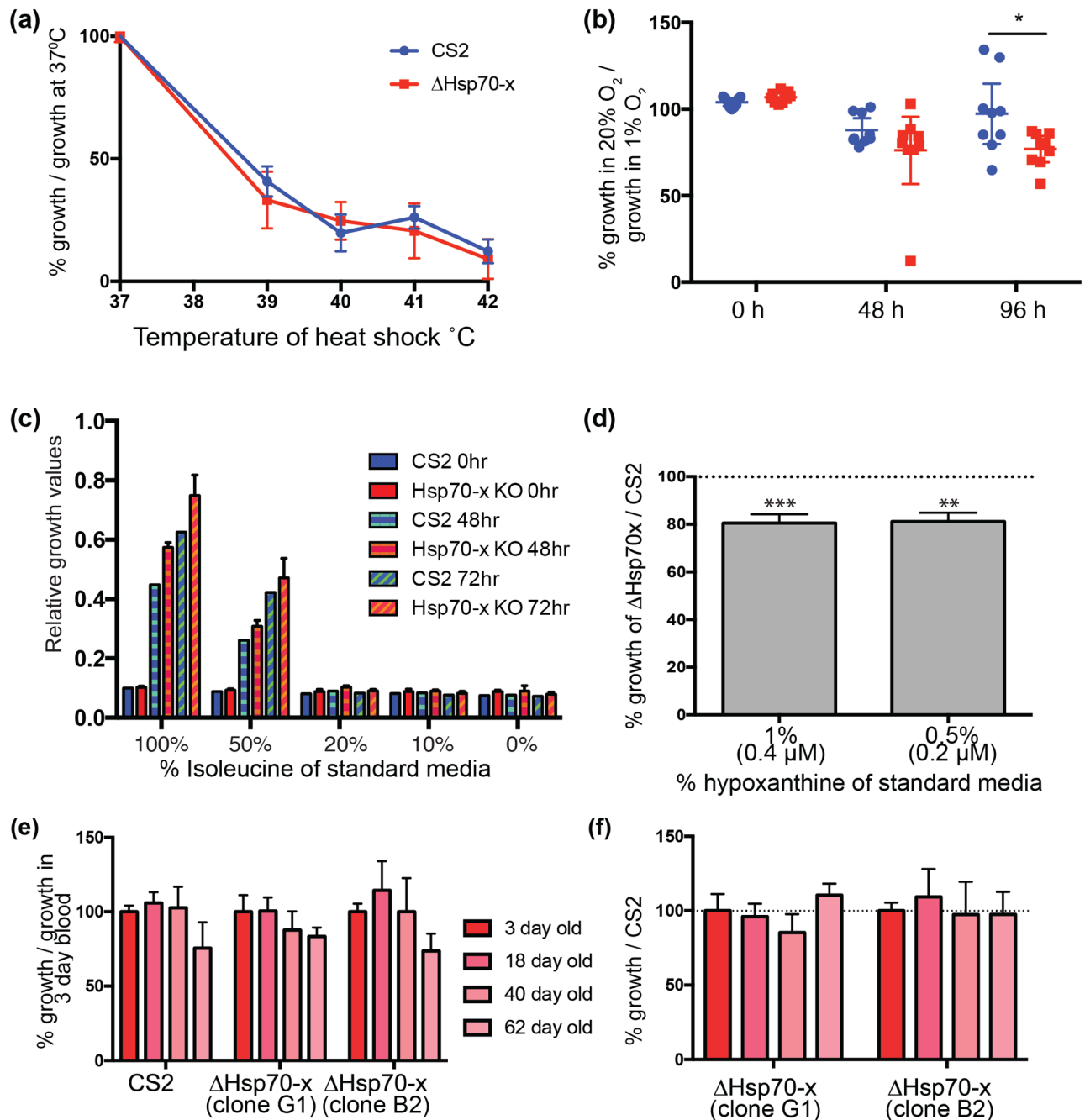


Fig 3. Δ Hsp70-x parasites generally resist stress as well as CS2. (a) Growth of Δ Hsp70-x and CS2 parasites for 1.5 cell cycles after heat shock treatment of ring stage parasites indicated that growth of the mutant Δ Hsp70-x and CS2 were similarly reduced. The ring-stage parasites were heat shocked at indicated temperatures for six hours and the percentage growth relative to parasite growth at 37°C is shown. The parasite lactate dehydrogenase (LDH) assay was used to measured growth and was performed twice in triplicate. (b) Percentage of blood stage parasite growth in 5% CO₂ in normal air (20% O₂) as a proxy for oxidative stress, relative to non-stressed cultures in 5% CO₂, 1% O₂. Both CS2 and Δ Hsp70-x have reduced growth in oxidative stress conditions at 48 h with Δ Hsp70-x not recovering as well as some of the CS2 replicates at 96 h. Growth was measured by LDH assay and performed in triplicate, showing the mean with 95% CI * p = 0.02. (c) Growth in media with reduced levels of isoleucine as measured by LDH assay at 0, 48 and 72 h after start of growth period, n = 2. For most isoleucine concentrations there was no difference between the Δ Hsp70-x and CS2 parasites. (d) With hypoxanthine reduced to 1% (0.4 μ M) and 0.5% (0.2 μ M) of standard RPMI culture conditions, the growth of Δ Hsp70-x was slightly reduced compared to CS2 as indicated by the dashed line at 100% (n = 3). Growth was measured by LDH activity after two cycles and was performed with two clones of Δ Hsp70-x whose data were combined because they were not significantly different to each other. T-test comparing Δ Hsp70-x growth to CS2 p = *** > 0.0001, ** 0.0008. (e) Growth of parasite lines in different aged erythrocytes as measured by LDH activity after 2.5 cell cycles indicates both parasite

lines grew less well in older erythrocytes. The erythrocytes were stored at 4°C for the indicated number of days prior to start of the assay. Parasite LDH was measured five days after the start of the assay and is reported as % growth compared to parasites grown in 3 day old blood, $n = 6$. (f) Data from (e) showing the growth of Δ Hsp70-x clones compared to control CS2 parasites normalised to 100% for each erythrocyte age group indicates no difference.

<https://doi.org/10.1371/journal.pone.0181656.g003>

compared. Parasites prefer a low oxygen environment and LDH assays performed after 48 hours incubation in these atmospheres indicated both parasites grew less well in 20% O₂ (Fig 3b). After 96 h in 20% O₂, growth continued to be reduced in both lines but CS2's growth had become variable between replicates (Fig 3b). It was possible that in some replicates CS2 was able to adapt to high O₂ conditions, whereas the Δ Hsp70-x line was not.

Next, we subjected the parasites to restriction of nutrients normally acquired from human blood plasma via new permeability pathways (NPPs). NPPs are broad specificity anion channels of the erythrocyte membrane permeable to amino acids, purines and vitamins and may be formed by secreted and exported parasite protein as well as co-opting human proteins [13, 44–46]. With Hsp70-x residing in the PV and erythrocyte compartments, this chaperone could be involved in the establishment or efficient functioning of NPPs. We compared the growth of Δ Hsp70-x and CS2 parasites in media depleted of two serum nutrients shown to be acquired via NPPs and essential for growth; isoleucine and hypoxanthine [47–49]. Isoleucine restriction was detrimental to both parasite lines, to an equivalent level, with neither line proliferating in 20% or less of standard culture media (Fig 3c). Hypoxanthine restriction to normal plasma levels [50] of 0.4 μ M (1% of standard culture media) or 0.2 μ M (0.5%) resulted in reduced growth of Δ Hsp70-x clones by 20% compared to CS2 (Fig 3d).

Finally we subjected the parasites to stress by culturing them in aged erythrocytes, which have reduced intrinsic chaperone activity, to determine whether host Hsp70s might be compensating for the loss of *P. falciparum* Hsp70-x (34). Parasite growth was measured by LDH assay in erythrocytes that had been previously stored at 4°C for 3 to 62 days. Although the growth rates of both lines were reduced in older erythrocytes (Fig 3e), there was no difference between two clones of Δ Hsp70-x and CS2 when the erythrocytes were matched for age (Fig 3f). The data indicate that although parasite growth is slightly reduced in aged erythrocytes, loss of Hsp70-x did not put the parasites at a significant growth disadvantage relative to CS2.

Δ Hsp70-x parasites have reduced virulence phenotypes with less efficient PfEMP1 export and cytoadherence

As the only exported chaperone of its class, Hsp70-x may also be necessary for the efficient export and function of *P. falciparum* proteins trafficked to and through the erythrocyte cytoplasm. Hsp70-x could be particularly important for the large *Laverania*-specific EMP1 virulence proteins which aid cytoadherence of IE, but are not necessary for *in vitro* culture [2]. PfEMP1 is first exported out of the parasite, across the PVM into the erythrocyte cytosol and then, via membranous lamellae called Maurer's clefts, is transferred onto knobs at the erythrocyte surface [51]. To determine the efficiency of exposure of PfEMP1 on the IE surface, whole IE were exposed to malaria immune sera from pregnant women [12, 29]. Since the majority of antibodies to the CS2 IE surface are targeted to the VAR2CSA PfEMP1 [30, 52] antibody binding to IE can therefore be used as a surrogate for PfEMP1 exposure on the surface. Antibody binding to the surface of Δ Hsp70-x IEs compared to CS2 was reduced by 32% at 26–28 hpi, but became nearly equal at 32–34 hpi. This suggested that PfEMP1 trafficking was slower and less efficient in Δ Hsp70-x, but ultimately surface exposed PfEMP1 reached similar levels in Δ Hsp70-x as CS2 (Fig 4a).

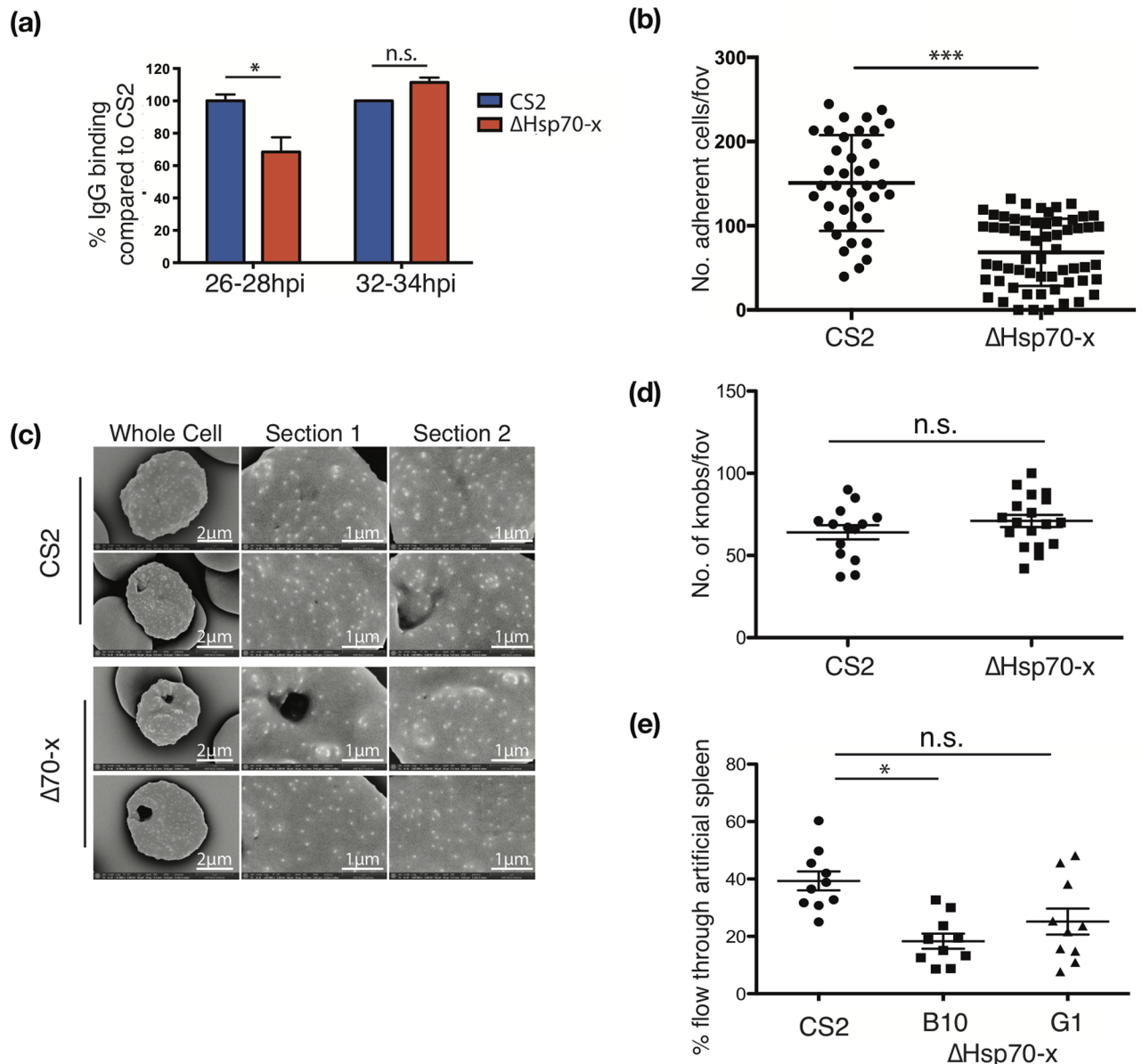


Fig 4. Δ Hsp70-x parasites export *PfEMP1* less efficiently, bind less well under flow and have altered cell rigidity. (a) Recognition of surface exposed *PfEMP1* by human immune sera indicates there is a delay in the deployment of *PfEMP1* on the surface of young (26–28 hpi) but not older (32–34 hpi) Δ Hsp70-x infected erythrocytes compared to CS2. Flow cytometry was used to measure the mean fluorescence intensity of *PfEMP1* on synchronized parasites and was performed in triplicate. T-test * $p = 0.04$, $n = 2$. (b) Cytoadhesion of infected cells at 32–34 hpi under a 0.05 Pa flow rate to simulate microvasculature conditions indicates that Δ Hsp70-x bind significantly less well than CS2. Adhesion was measured as the mean number of cells/view, dot plot shows CS2 geometric mean of 138, Δ Hsp70-x geometric mean of 51 in three clones, indicating an overall reduction in binding of 63%. Wilcoxon test *** $p < 0.0001$ $n = 3$, each performed in triplicate. (c) Representative scanning electron micrographs of CS2 and Δ Hsp70-x infected erythrocytes indicate similar morphology and density of knobs. (d) Analysis of number of knobs per field of view of single IE CS2 and Hsp70-x shows no significant difference. (e) Deformability of infected erythrocytes (23–26 hpi) measured by reduced passage through an artificial spleen system of packed micro-beads. The Δ Hsp70-x clone B10, is more rigid than CS2 (T-test CS2 v B10 * $p = 0.03$). Clone G1 also more rigid than CS2 but not significantly so (CS2 v G1 $p = 0.11$). $n = 3$, each performed in triplicate.

<https://doi.org/10.1371/journal.pone.0181656.g004>

Efficient cytoadherence to endothelial cells depends on a number of factors, including the surface exposure of *PfEMP1* on correctly formed knob structures and the increased rigidity of the IE cytoskeleton [5, 31, 53–55]. The CS2 parasite line in which the Δ Hsp70-x clones were derived from stably expresses the single VAR2CSA *PfEMP1* allele, which binds to chondroitin

sulfate A (CSA) normally present in the placenta [56]. In static conditions Δ Hsp70-x and CS2 were equally able to bind to immobilised CSA (Figure A in S1 Fig). However under flow conditions of 0.05 Pa, a similar flow rate as may be experienced in placental microvasculature, Δ Hsp70-x binding was reduced by 63% (Fig 4b) [57, 58]. These assays were performed at 32–36 hpi, when *Pf*EMP1 surface expression was equivalent between the knockout and control lines (Fig 4a). At higher flow rates (0.1 Pa) both CS2 and Δ Hsp70-x lines were unable to efficiently bind CSA (Figure B S1 Fig). A decrease in cytoadherence of Δ Hsp70-x IE under flow could be due to incorrect loading of *Pf*EMP1 into knobs, or the incorrect formation of knob structures to efficiently display *Pf*EMP1. Scanning electron microscopy was performed to examine knob morphology and revealed that both lines produced knobs, and there were no obvious morphological differences in the size and density of knobs between the lines (Fig 4c and 4d).

As knob formation and *Pf*EMP1 surface exposure appears to be similar between CS2 and Δ Hsp70-x, yet cytoadherence was reduced, we therefore investigated another factor related to efficient cytoadherence; the rigidity of the IEs. An artificial spleen model mimicking splenic slits measures the ability of the IE to deform as they traverse through a bed of packed 5–25 μ M microbeads [32]. Δ Hsp70-x IE traversed the bead-bed less efficiently over the measurement period than age-matched CS2 parasites (Fig 4e). At 25–29 hpi 40% of CS2 parasites traversed the spleen, yet for two Δ Hsp70-x clones only 18% and 25% traversed, respectively. Older 28–32 hpi parasites from both lines were unable to traverse the bead bed due to increased rigidity (data not shown). The data indicate that the Δ Hsp70-x IE become more rigid at an earlier point in the intraerythrocytic developmental cycle than CS2. Collectively, the decrease in rate of surface exposure of *Pf*EMP1 and increased stiffness of the IE membrane in Δ Hsp70-x may be the cause of reduced CSA binding under flow.

Increased expression of exported proteins may be compensating for the loss of Hsp70-x

With the loss of Δ Hsp70x expression causing a reduction in cytoadherence and increased stiffness of the IE we examined whether these effects were due to changes in the expression of other exported proteins. Such compensatory changes may have occurred during the generation of the knockout line to counter the loss of Hsp70-x, and uncovering such compensation may help indicate the function of Hsp70-x. As a first method to quickly compare the levels of exported protein in Δ Hsp70-x and CS2, immunofluorescence microscopy was performed on highly synchronized parasites. Each line was imaged with the same exposure settings and the mean fluorescence intensity (MFI) of individual cells labeled with antibodies to different exported proteins was measured. Antibodies to the cytoskeletal binding proteins ring exported surface antigen (RESA) and knob associated histidine rich protein (KAHRP) indicated the MFI was significantly higher for KAHRP but not RESA in the mutant (Fig 5a and 5b). Western blot analysis was also performed for KAHRP and RESA as well as exported protein skeleton binding protein 1 (SBP1) which is required for *Pf*EMP1 export, and localises to Maurer's clefts [59]. As the timing of the expression of these proteins is different, mixed ring and trophozoite stage parasites were used. The culture was magnet purified to separate the rings from the trophozoites which were saponin treated to remove haemoglobin or fractionated as whole cells, respectively. By eye, ring-stage KAHRP appeared to be expressed at slightly higher levels in the two Δ Hsp70-x lines (Fig 5c). Densitometry also supported this result however after normalizing for Hsp70-1 and EXP2 the trend was not significant ($p = 0.1$, Fig 5d). Densitometry of RESA and SBP1 were unchanged in the mutants. The trend towards increased KAHRP expression in Δ Hsp70-x IE suggested these and possibly other exported proteins might be up-regulated in Δ Hsp70-x parasites.

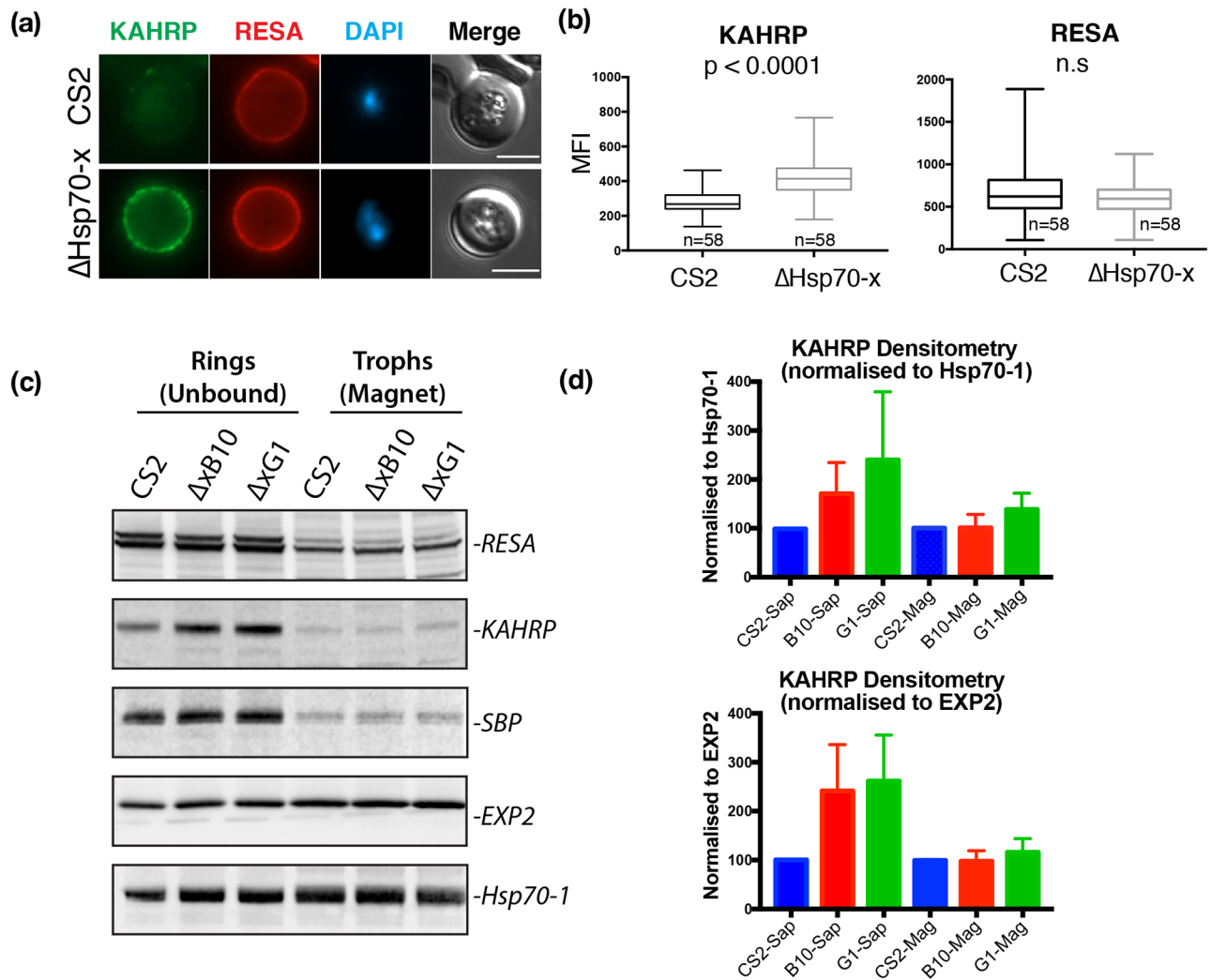


Fig 5. The expression of cytoskeletal binding proteins KAHRP is increased in Δ Hsp70-x. (a) Immunofluorescence microscopy of 16-24hpi parasites indicates expression of the exported, knob localized KAHRP protein but not RESA appears higher in Δ Hsp70-x. n = number of cells counted. (b) Mean fluorescence intensity (MFI) measurements of the erythrocyte compartment confirmed the KAHRP signal is higher in Δ Hsp70-x compared to CS2 (Mann Whitney test). (c) Western blot analysis of magnet binding (trophozoites) and unbound (ring stage) parasites indicates KAHRP but not RESA or SBP1 appears to be more highly expressed in two Δ Hsp70-x clonal lines. Whole purified trophozoites and saponin treated ring stage parasites were analyzed. (d) Densitometry of KAHRP levels from three blots normalized to Hsp70-1 and EXP2 loading controls, indicated that although KAHRP expression was always higher in Δ Hsp70-x than CS2 this was not significant ($p = 0.1$, pairwise comparison, Mann Whitney test).

<https://doi.org/10.1371/journal.pone.0181656.g005>

For a comprehensive analysis of exported protein levels a quantitative proteomic approach, Stable Isotope Labeling with Amino acids in Cell culture (SILAC), was used to identify up- and down-regulated proteins in Δ Hsp70-x parasites compared to CS2. Δ Hsp70-x parasite proteins were labeled with heavy (^{13}C and ^{15}N) isoleucine and CS2 with light isoleucine, and samples were mixed, purified and analysed together. Exported proteins were enriched, by using equinotoxin to perforate only the erythrocyte membrane and to release soluble exported proteins. Lysis and centrifugation also released membranous structures in the host cell, and fragments of erythrocyte membrane and associated proteins. Haemoglobin was removed by passing the samples over nickel resin, which also removed histidine rich proteins. The ratio of Heavy/Light for individual peptides was normalized to the vast majority of proteins that were

present at a 1:1 ratio, represented at the base of the 'volcano plot' in Fig 6a. A total of 304 proteins were identified and individual proteins identified as up- (upper right) or down- (upper left) regulated in Δ Hsp70-x parasites constituted minor subsets (Fig 6a and S1 and S2 Tables). Only two exported proteins RESA (PF3D7_0102200) and a PEXEL-containing uncharacterised protein (PF3D7_0501000), exceeded both P-value and Z-score parameters for up-regulation in Δ Hsp70-x (red spots, Fig 6a and 6d and S1 and S2 Tables). Of the four other proteins that exceeded at least one parameter, two were exported (PF3D7_1353200 and PF3D7_0532400) and two were chaperones located within the parasite (yellow spots, Fig 6a and 6d and S1 and S2 Tables). Within the top twenty proteins with H/L ratios >1.25 , were also two other chaperones and at least three exported proteins (S1 and S2 Tables).

In contrast to the relatively few proteins over-expressed in Δ Hsp70-x, there were many more under-expressed relative to CS2 (Fig 6a, S1 and S2 Tables). There were 16 under-expressed proteins that exceeded both Z-score and P-value parameters and twice as many proteins that exceeded a single parameter (red and yellow spots, respectively, Fig 6a). Hsp70-x peptides were amongst those under-represented in the Δ Hsp70-x parasites (Fig 6a, S1 and S2 Tables). In theory there should be no peptides in Hsp70-x parasites but since this protein is very similar to the cytoplasmic chaperone Hsp70-1 [18], a few peptides of the cytoplasmic chaperone may have been counted as being from the exported chaperone. Many of the proteins under-expressed in Δ Hsp70-x trophozoites were schizont proteins (eg, rhoptry proteins [RAPs and RhopHs] and merozoite surface proteins [MSPs]).

As both the immunofluorescence and proteomics approaches examined surface and exported proteins in trophozoites, we used RNA-seq to investigate the effects of Δ Hsp70-x deletion upon steady-state mRNA levels in tightly synchronized ring, trophozoite and schizont stage parasites. Expression of most genes was closely correlated at each time point, indicating close age-matching of replicates (Pearson correlation coefficient >0.9) (Fig 6b). Each sample also correlated well to the expected time points of the intra-erythrocytic development cycle derived from published microarray data [60] (S2 Fig). The greatest number of differentially expressed genes detected between the two parasite lines occurred at the trophozoite stage. Differences in read counts and fold change are illustrated in Fig 6c; differentially expressed genes are highlighted in red (Fig 6c, S3 Table). Of the small number of up-regulated Δ Hsp70-x genes identified in trophozoites and schizonts the majority of these (8/9 at trophozoite, 3/7 at schizont) were predicted to be exported (Fig 6d and S1 and S3 Tables). In comparison, many more genes were identified as down-regulated in Δ Hsp70-x trophozoites compared to CS2 (S1 and S3 Tables). The majority of these down-regulated genes encode known schizont stage proteins, involved in processes such as invasion.

Discussion

Hsp70-x, which localises to the PV and is exported into the host cell via PTEX, is the only known *Plasmodium* exported Hsp70 [18, 61]. Hsp70-x is present only in the *Laverania* subgenus, which have three major features in common; 1) they infect erythrocytes of all ages, 2) they encode an EMP1 type protein used for cytoadherence in *P. falciparum*, and 3) they have large exportomes. We show here that Hsp70-x can be deleted *in vitro*, and the resulting mutant parasites are still able to export PfEMP1, but the process is less efficient and the resulting IE are less cytoadherent and more rigid. Decreased binding in the microvasculature and increased rigidity of these parasites should lead to enhanced splenic clearance, which we recapitulate using an *in vitro* model indicating Δ Hsp70-x could be important *in vivo*. The deletion of Δ Hsp70-x appears to trigger multiple changes in the transcription and translation of exported proteins in particular, which could in part compensate for the loss of this chaperone. We

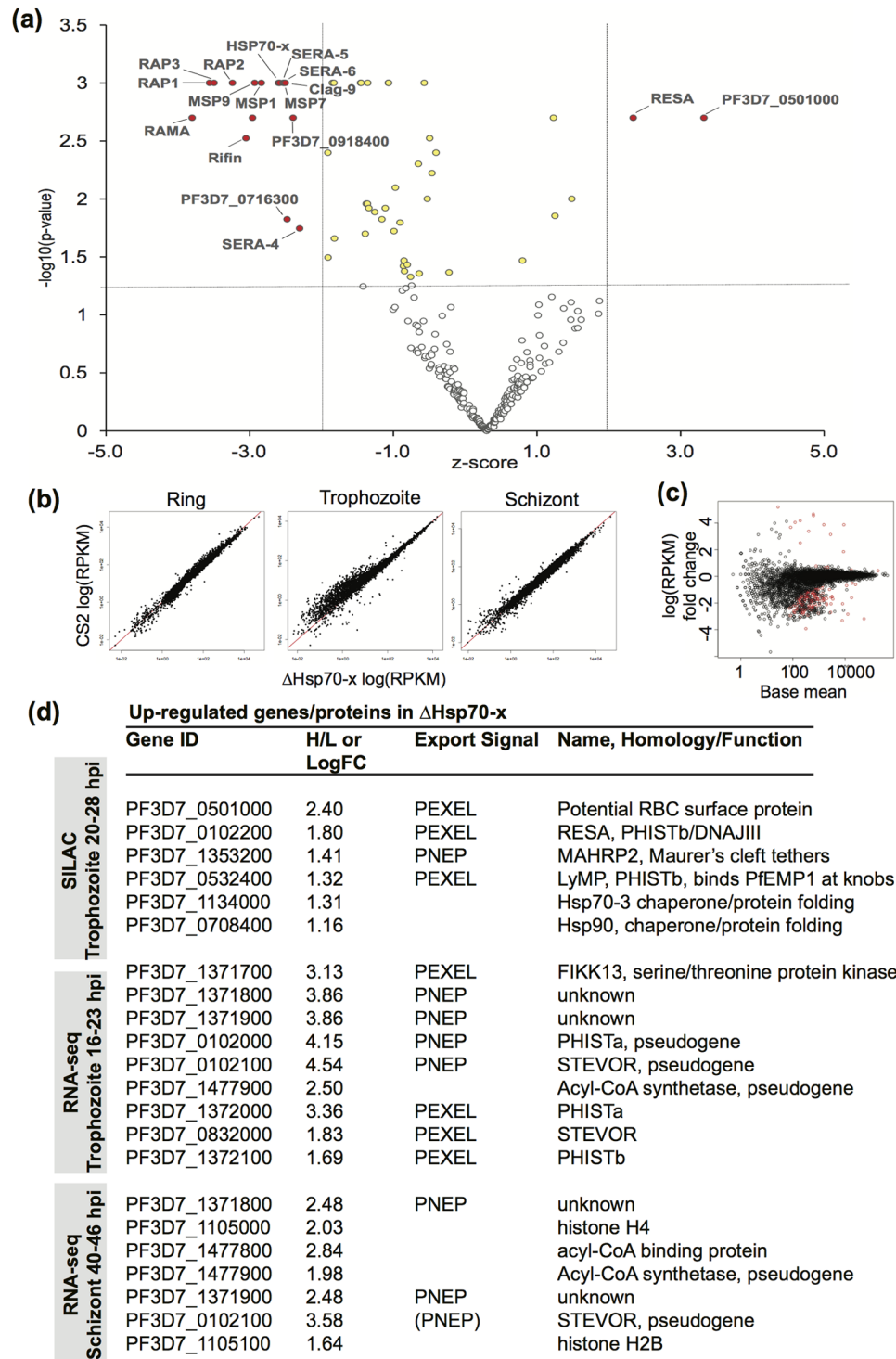


Fig 6. Transcriptional and translational changes in $\Delta\text{Hsp70-x}$ indicate an up-regulation of some exported proteins. (a) Mass spectrometry based SILAC sequencing of proteins indicates several exported proteins are over- and under-expressed in $\Delta\text{Hsp70-x}$ relative to CS2. $\Delta\text{Hsp70-x}$ and CS2 were differentially labeled with heavy (H) and light (L) isotopic forms of isoleucine respectively. Proteins with statistically insignificant Z-score ratios (X-axis) versus $-\log_{10}(\text{P-value})$ (Y-axis) and therefore in ~ 1:1 ratio represent the base of the volcano plot. Proteins at higher levels in $\Delta\text{Hsp70-x}$ only and which satisfy both statistical parameters are labeled in red in the upper right. Those up-regulated proteins that only satisfy one parameter are labeled in yellow. Proteins down-regulated in $\Delta\text{Hsp70-x}$ are similarly coloured and shown in the upper left.

(b) Correlation plots of RNA-seq transcripts between wild type and Δ Hsp70-x ring, trophozoite and schizont stages show close correlation in most transcripts (close to line $x = y$). Most differential genes are downregulated in Δ Hsp70-x trophozoites and schizonts (points furthest from line). (c) MA plot representing RNA-seq data. The change in expression (\log_2 fold change) is plotted against the average of the normalized count values (base mean), of Δ Hsp70-x and CS2 transcripts at the trophozoite stage. Red dots indicate differentially expressed genes in Δ Hsp70-x. (d) Summary of increased proteins and transcripts by SILAC and RNA-seq. Numbers indicate heavy/light isoleucine ratio (H/L) in SILAC ordered by the ratio, or the \log_2 fold change in transcripts (LogFC) in RNA-seq data, ordered by significance which takes into account number of transcripts as well. Exported proteins are denoted as PEXEL or no PEXEL (PNEP) or otherwise left blank. Known homology to protein families or potential function identified in final column, including annotated pseudogenes. Pseudogenes may produce a limited numbers of transcripts so small changes can look significant.

<https://doi.org/10.1371/journal.pone.0181656.g006>

acknowledge these changes could also be partly a result of the clonal selection process used to isolate the Δ Hsp70-x parasites that may have other mutations but the fact that multiple clones performed similarly makes this less likely. The data therefore indicate that although Hsp70-x is not essential for growth it may aid in the efficient export or function of some proteins that are important *in vivo*. To overcome possible adaptive processes using the knock out approach we attempted to rapidly knockdown Hsp70-x by integrating a riboswitch *glmS* into the 3'UTR. Surprisingly there was no significant protein knockdown following glucosamine treatment, and so we have not included these experiments.

Hsp70-x is located in the subtelomeric region of chromosome 8, and in a study of Peruvian clinical isolates loss of the adjacent gene histidine-rich protein 2 (*hrp2*) occurred in 40.5% of isolates but only 11.5% lacked *hsp70-x* [62]. This suggests the biological role for Hsp70-x *in vivo* is important as few isolates lose this gene even when neighboring genes are lost. Growth responses to multiple stressors were analysed and identified little change in Δ Hsp70-x.

Hsp70-x may play a role in immune evasion, specifically in PfEMP1 export and cytoadherence. Lack of Hsp70-x delayed but did not prevent exposure of PfEMP1 on the surface of the iRBC as measured by reaction to human immune sera and cytoadhesion under static conditions. However, under low-pressure flow conditions reminiscent of flow rates in the placenta, Δ Hsp70-x IE were significantly less able to cytoadhere to CSA compared to CS2 at an intra-erythrocytic time point where both lines had equal levels of surface-exposed PfEMP1. Neither parasite line was able to efficiently cytoadhere under high flow conditions, indicative of the reduced cytoadhesive properties of placental binding parasites such as CS2 in general [63]. We do not believe reduced cytoadherence is due to a sub-population of slower developing parasites in Δ Hsp70-x as we performed the experiments when equal amounts of surface exposed PfEMP1 are present, and we see no evidence of two populations one more delayed than the other, nor in the cytoadherence and cellular rigidity. Slower delivery of PfEMP1 to the surface may be due to reduced export efficiency although a less synchronous Δ Hsp70-x population could also be contributing (see below). Slower PfEMP1 export may also be due to disruption of J-dots, chaperone dense regions that contain Hsp70-x and colocalise with PfEMP1 during its export to the cell surface [18] which warrants further study.

Cytoadherence can be affected by knob formation and/or cytoskeletal changes in the erythrocyte induced by parasite derived proteins. Although Δ Hsp70-x IE parasites appeared to have normal knob density, they were retained more efficiently in an artificial spleen model, indicating increased rigidity. In the presence of functioning PfEMP1 increased stiffness leads to increased cytoadhesion [64], however in the absence of functional surface PfEMP1 increased stiffness would further reduce cytoadherence and lead to enhanced clearance by the immune system *in vivo*. Deletion of some exported proteins is known to decrease the rigidity of the RBC membrane [5], and therefore increased expression of these proteins might be expected to escalate membrane rigidity. This was supported by microscopy of the spectrin-

binding KAHRP in Δ Hsp70-x parasites which indicated it was over-expressed relative to CS2, and thus may be contributing to increased rigidity. We note however that although not specifically measured, the knobs of Δ Hsp70-x appeared normal despite higher KAHRP expression.

To obtain a broader picture of altered protein expression in Δ Hsp70-x IE, mass spectrometry based protein quantification of exported proteins was performed. The data was enriched for exported proteins by erythrocyte membrane lysis with equinatoxin, which also identified cytoskeleton binding proteins. This is probably due to small light weight membrane fragments remaining in the supernatant. Quantitative SILAC analysis identified RESA and a protein of unknown function with high confidence, although analysis was only performed once. The increase in RESA levels by SILAC was not supported by microscopy and western blots. RESA's increase by SILAC could be due to increased solubility and release from the cytoskeleton in Δ Hsp70-x trophozoites. PF3D7_0501000 is predicted to be exported and may be on the iRBC surface [65] although we do not have antibodies available to confirm elevated levels in Δ Hsp70-x. KAHRP, being rich in histidine residues, was probably lost during the nickel bead step used to remove hemoglobin and was not detected. Other over-expressed proteins were MAHRP2 (PF3D7_1353200) and LyMP, (PF3D7_0532400) which have been shown to respectively help tether Maurer's clefts to the erythrocyte surface, and the ATS of certain *PfEMP1* to the cytoskeleton [66–68]. Over-expression of these cytoskeleton binders could also have contributed to the increased rigidity [64].

Since the proteomics approach was enriched for exported trophozoite proteins we employed RNA-seq to investigate genome-wide changes in the major asexual blood developmental stages of the parasite; rings, trophozoites and schizonts. Relative to CS2, genes up-regulated in Δ Hsp70-x encode several exported proteins in both the trophozoite and schizont stages. Like LyMP, many of the genes with up-regulated transcripts encode exported proteins with PHIST (*Plasmodium* helical interspersed sub-telomeric) domains; these proteins may bind and modify the erythrocyte's cytoskeleton [68]. The most up-regulated gene in Δ Hsp70-x trophozoites was the exported kinase FIKK13 [69, 70]. The function of FIKK13 is unknown but it may have a role in cytoadherence and/or membrane rigidity as knockouts of the exported FIKK4.2 and FIKK12 kinases affect these phenomena [71, 72]. We note with RESA, that an increase in transcript levels did not produce a rise in protein abundance by microscopy and western blot and so whether or not a gene upregulated by RNA-seq leads to increased protein levels will need to be validated for each gene.

Although we carefully attempted to age match Δ Hsp70-x and CS2 trophozoites and schizonts there were a number of transcripts and proteins identified as down expressed by RNA-seq and SILAC. These tended to be for late stage invasion proteins and it is possible that Δ Hsp70-x parasites were slightly less synchronous than CS2 meaning the proportion of older parasites was a little lower in Δ Hsp70-x. The mutant may have been more difficult to synchronize by sorbitol because their NPPs were less active. The fact that Δ Hsp70-x was slightly more sensitive to restriction of imported hypoxanthine suggests further evaluation of NPP function is warranted.

Hsp70-x would be expected to have a diverse set of binding partners due to its dual location in the PV and in the host cytosol [16, 18]. To further understand Hsp70-x's function we attempted to directly identify its client proteins by immunoprecipitation with IgG raised to the less conserved peptide binding and 'lid' regions of Hsp70-x to prevent cross reactivity with other parasite Hsp70s. This approach however failed to identify strong binding partners possibly because the IgG was competing for the same binding site as the chaperone's client proteins. Immunoprecipitation of the PTEX subunits PTEX150, EXP2 and Hsp101 does co-purify Hsp70-x suggesting it may be assisting Hsp101 to unfold cargo or might be cargo itself [12, 17, 61]. In silico modeling has suggested that Hsp70-x may bind a range of Hsp40s [73], and

chaperone rich J dots containing both Hsp70-x and two Hsp40s have been identified [18]. It has recently also been suggested that host Hsp70s can bind to parasite derived Hsp40s [74] supporting the idea that Hsp70-x is not the only Hsp70 co-opted by the parasite for functions in the host cell, however it is the only parasite derived Hsp70 present in the host cell.

Conclusions

We show that Hsp70-x is not necessary for survival of *P. falciparum* in mature erythrocytes and is not essential for export of PfEMP1. Our data support the hypothesis that Hsp70-x assists efficient export and functioning of some exported proteins that contribute towards virulence. Δ *hsp70-x* parasites have undergone a large number of gene regulatory changes that may be compensatory, and have resulted in mild but significant phenotypes such as slower export of PfEMP1, reduced cytoadherence and increased erythrocyte rigidity. By enhancing large-scale protein export Hsp70-x may contribute to the virulence of *Laverania* parasites in their primate hosts.

Supporting information

S1 Fig. Cytoadhesion in static and flow conditions. (a) Static adhesion of IE to CSA bound to plastic dish. Measured by light microscopy of number of IE/mm², $n = 3$, no statistical difference between lines. (b) Cytoadhesion of infected cells at 32–34 hpi under a 0.05 Pa and 0.1 Pa flow rate. Adhesion was measured as the mean number of cells/view, box interquartile range and whiskers min-max, $n = 3$, each performed in triplicate.

(PDF)

S2 Fig. RNA-seq correlation with microarray data indicating close age matching. Correlation plot of normalized expression values (RPKM) against microarray data [60] shows good correlation between biological replicates and between wild type and Δ Hsp70-x. Schizont samples have some correlation with ring stage microarray transcripts as expected. WT indicates CS2 and KO indicates Δ Hsp70-x, two biological replicates performed at each time point (rings, trophozoites and schizonts). V indicates time points taken post invasion in [60].

(PDF)

S1 Table. List of all differentially expressed proteins and transcripts identified by SILAC and RNA-seq. Homology, function and export of proteins and genes identified are those corresponding to PlasmoDB Release 29. Proteins are identified being EXPORTED if they contain a PEXEL sequence, or PNEP if known to be exported but lacking a PEXEL sequence. SILAC proteins were designated up-regulated if H/L ratio ≥ 1.25 and down-regulated if ≤ 0.75 . Proteins are color coded as per Fig 6 and the number of H and L peptide pair observations are indicated. For RNA-seq, maximal expression at stage sampled determined to be “yes” transcription was 24–36 hpi for trophozoites or 36–0 hpi for schizonts as determined from data available from PlasmoDB. RNA-seq downregulated trophozoite proteins only showing top hits, full data in S3 Table.

(XLSX)

S2 Table. Total proteomics data for SILAC analysis.

(XLSX)

S3 Table. Total RNA-seq data for all genes in each biological replicate. CS2 (WT) and Δ Hsp70-x (KO) synchronised with sorbitol to within 8 hours window and grown separately for at least three cycles to get biological replicates 1 and 2 at three life stages; rings, trophozoites (trophs) and schizonts (schiz). Tab1 indicates RPKM, Tab2 indicates Degust differential

expression analysis of WT and KO trophozoite stage shown with false discovery rate (FDR). (XLSX)

Acknowledgments

We thank A. Cowman, B. Cooke, and R. Anders for reagents and/or other assistance with aspects of this study; D. Staniscic, F. Baiwog and I. Mueller for contributions to clinical studies of pregnant women; and P. Siba. We also thank the Australian Red Cross Blood Service for supply of red blood cells and human serum, and Monash Micro Imaging for technical assistance with microscopy.

Author Contributions

Conceptualization: Sarah C. Charnaud, Jude M. Przyborski, Brendan S. Crabb, Paul R. Gilson.

Data curation: Sarah C. Charnaud, Matthew W. A. Dixon, Lia Chappell, Thomas Nebl.

Formal analysis: Sarah C. Charnaud, Matthew W. A. Dixon, Catherine Q. Nie, Lia Chappell, Paul R. Sanders, Thomas Nebl, Eric Hanssen, Paul R. Gilson.

Funding acquisition: James G. Beeson, Julian C. Rayner, Leann Tilley, Brendan S. Crabb, Paul R. Gilson.

Investigation: Sarah C. Charnaud, Matthew W. A. Dixon, Catherine Q. Nie, Paul R. Sanders, Thomas Nebl, Adam J. Blanch, Paul R. Gilson.

Methodology: Sarah C. Charnaud, Matthew W. A. Dixon, Paul R. Sanders, Thomas Nebl, Eric Hanssen, Matthew Berriman, Jo-Anne Chan, Adam J. Blanch, Jude M. Przyborski, Paul R. Gilson.

Project administration: Sarah C. Charnaud, Paul R. Gilson.

Resources: Matthew Berriman, Jo-Anne Chan, James G. Beeson, Julian C. Rayner.

Software: Lia Chappell, Matthew Berriman.

Supervision: Matthew Berriman, Julian C. Rayner, Leann Tilley, Brendan S. Crabb, Paul R. Gilson.

Validation: Sarah C. Charnaud, Paul R. Gilson.

Visualization: Sarah C. Charnaud.

Writing – original draft: Sarah C. Charnaud, Paul R. Gilson.

Writing – review & editing: Sarah C. Charnaud, Jude M. Przyborski, Leann Tilley, Paul R. Gilson.

References

1. World Malaria Report [Internet]. 2016.
2. Newbold C, Craig A, Kyes S, Rowe A, Fernandez-Reyes D, Fagan T. Cytoadherence, pathogenesis and the infected red cell surface in *Plasmodium falciparum*. *Int J Parasitol*. 1999; 29(6):927–37. PMID: [10480730](https://pubmed.ncbi.nlm.nih.gov/10480730/).
3. Rogerson SJ, Hviid L, Duffy PE, Leke RF, Taylor DW. Malaria in pregnancy: pathogenesis and immunity. *Lancet Infect Dis*. 2007; 7(2):105–17. [https://doi.org/10.1016/S1473-3099\(07\)70022-1](https://doi.org/10.1016/S1473-3099(07)70022-1) PMID: [17251081](https://pubmed.ncbi.nlm.nih.gov/17251081/).

4. Umbers AJ, Aitken EH, Rogerson SJ. Malaria in pregnancy: small babies, big problem. *Trends Parasitol.* 2011; 27(4):168–75. <https://doi.org/10.1016/j.pt.2011.01.007> PMID: 21377424.
5. Maier AG, Rug M, O'Neill MT, Brown M, Chakravorty S, Szeszak T, et al. Exported Proteins Required for Virulence and Rigidity of *Plasmodium falciparum*-Infected Human Erythrocytes. *Cell.* 2008; 134(1):48–61. <https://doi.org/10.1016/j.cell.2008.04.051> PMID: 18614010
6. Crabb BS, de Koning-Ward TF, Gilson PR. Protein export in *Plasmodium* parasites: from the endoplasmic reticulum to the vacuolar export machine. *International Journal For Parasitology.* 2010; 40(5):509–13. <https://doi.org/10.1016/j.ijpara.2010.02.002> PMID: 20170656. Date Created: 20100326. Date Completed: 20100607. Update Code: 20101124. Publication Type: Journal Article.
7. Gehde N, Hinrichs C, Montilla I, Charpian S, Lingelbach K, Przyborski JM. Protein unfolding is an essential requirement for transport across the parasitophorous vacuolar membrane of *Plasmodium falciparum*. *Molecular Microbiology.* 2009; 71(3):613–28. <https://doi.org/10.1111/j.1365-2958.2008.06552.x> PMID: 19040635
8. de Koning-Ward TF, Gilson PR, Boddey JA, Rug M, Smith BJ, Papenfuss AT, et al. A newly discovered protein export machine in malaria parasites. *Nature.* 2009; 459(7249):945–9. <https://doi.org/10.1038/nature08104> PMID: 19536257. Date Revised: 20100927. Date Created: 20090618. Date Completed: 20090812. Update Code: 20101124. Publication Type: Journal Article.
9. Hiller NL, Bhattacharjee S, van Ooij C, Liolios K, Harrison T, Lopez-Estrano C, et al. A host-targeting signal in virulence proteins reveals a secretome in malarial infection. *Science.* 2004; 306(5703):1934–7. <https://doi.org/10.1126/science.1102737> PMID: 15591203
10. Marti M, Good RT, Rug M, Knuepfer E, Cowman AF. Targeting Malaria Virulence and Remodeling Proteins to the Host Erythrocyte. *Science.* 2004; 306(5703):1930–3. <https://doi.org/10.1126/science.1102452> PMID: 15591202
11. Heiber A, Kruse F, Pick C, Grüning C, Flemming S, Oberli A, et al. Identification of New PNEPs Indicates a Substantial Non-PEXEL Exportome and Underpins Common Features in *Plasmodium falciparum* Protein Export. *PLoS Pathogens.* 2013; 9(8):e1003546. <https://doi.org/10.1371/journal.ppat.1003546> PMID: 23950716
12. Elsworth B, Matthews K, Nie CQ, Kalanon M, Charnaud SC, Sanders PR, et al. PTEX is an essential nexus for protein export in malaria parasites. *Nature.* 2014; 511(7511):587–91. <https://doi.org/10.1038/nature13555> PMID: 25043043
13. Beck JR, Muralidharan V, Oksman A, Goldberg DE. PTEX component HSP101 mediates export of diverse malaria effectors into host erythrocytes. *Nature.* 2014; 511(7511):592–5. <https://doi.org/10.1038/nature13574> PMID: 25043010
14. Glover JR, Lindquist S. Hsp104, Hsp70, and Hsp40: a novel chaperone system that rescues previously aggregated proteins. *Cell.* 1998; 94(1):73–82. PMID: 9674429.
15. Seyffer F, Kummer E, Oguchi Y, Winkler J, Kumar M, Zahn R, et al. Hsp70 proteins bind Hsp100 regulatory M domains to activate AAA+ disaggregase at aggregate surfaces. *Nat Struct Mol Biol.* 2012; 19(12):1347–55. <https://doi.org/10.1038/nsmb.2442> PMID: 23160352.
16. Elsworth B, Sanders PR, Nebl T, Batinovic S, Kalanon M, Nie CQ, et al. Proteomic analysis reveals novel proteins associated with the *Plasmodium* protein exporter PTEX and a loss of complex stability upon truncation of the core PTEX component, PTEX150. *Cellular Microbiology.* 2016; 18:1551–69. <https://doi.org/10.1111/cmi.12596> PMID: 27019089
17. Zhang Q, Ma C, Oberli A, Zinz A, Engels S, Przyborski JM. Proteomic analysis of exported chaperone/co-chaperone complexes of *P. falciparum* reveals an array of complex protein-protein interactions. *Sci Rep.* 2017; 7:42188. <https://doi.org/10.1038/srep42188> PMID: 28218284.
18. Kulzer S, Charnaud S, Dagan T, Riedel J, Mandal P, Pesce ER, et al. *Plasmodium falciparum*-encoded exported hsp70/hsp40 chaperone/co-chaperone complexes within the host erythrocyte. *Cell Microbiol.* 2012; 14(11):1784–95. <https://doi.org/10.1111/j.1462-5822.2012.01840.x> PMID: 22925632.
19. Antinori S, Galimberti L, Milazzo L, Corbellino M. Biology of human malaria plasmodia including *Plasmodium knowlesi*. *Mediterr J Hematol Infect Dis.* 2012; 4(1):e2012013. <https://doi.org/10.4084/MJHID.2012.013> PMID: 22550559.
20. Sargeant T, Marti M, Caler E, Carlton J, Simpson K, Speed T, et al. Lineage-specific expansion of proteins exported to erythrocytes in malaria parasites. *Genome Biology.* 2006; 7(2):R12. <https://doi.org/10.1186/gb-2006-7-2-r12> PMID: 16507167
21. Otto TD, Rayner JC, Bohme U, Pain A, Spottiswoode N, Sanders M, et al. Genome sequencing of chimpanzee malaria parasites reveals possible pathways of adaptation to human hosts. *Nat Commun.* 2014; 5:4754. <https://doi.org/10.1038/ncomms5754> PMID: 25203297.
22. Larremore DB, Sundararaman SA, Liu W, Proto WR, Clauset A, Loy DE, et al. Ape parasite origins of human malaria virulence genes. *Nat Commun.* 2015; 6:8368. <https://doi.org/10.1038/ncomms9368> PMID: 26456841.

23. McQueen PG, McKenzie FE. Age-structured red blood cell susceptibility and the dynamics of malaria infections. *Proc Natl Acad Sci U S A*. 2004; 101(24):9161–6. <https://doi.org/10.1073/pnas.0308256101> PMID: 15178766.
24. Nosten F, McGready R, Simpson JA, Thwai KL, Balkan S, Cho T, et al. Effects of *Plasmodium vivax* malaria in pregnancy. *Lancet*. 1999; 354(9178):546–9. PMID: 10470698.
25. Simpson JA, Silamut K, Chotivanich K, Pukrittayakamee S, White NJ. Red cell selectivity in malaria: a study of multiple-infected erythrocytes. *Trans R Soc Trop Med Hyg*. 1999; 93(2):165–8. PMID: 10450440.
26. Trager W, Jensen J. Human malaria parasites in continuous culture. *Science*. 1976; 193(4254):673–5. <https://doi.org/10.1126/science.781840> PMID: 781840
27. Maier AG, Braks JA, Waters AP, Cowman AF. Negative selection using yeast cytosine deaminase/uracil phosphoribosyl transferase in *Plasmodium falciparum* for targeted gene deletion by double crossover recombination. *Mol Biochem Parasitol*. 2006; 150(1):118–21. <https://doi.org/10.1016/j.molbiopara.2006.06.014> PMID: 16901558.
28. Makler MT, Ries JM, Williams JA, Bancroft JE, Piper RC, Gibbins BL, et al. Parasite Lactate Dehydrogenase as an Assay for *Plasmodium falciparum* Drug Sensitivity. *The American Journal of Tropical Medicine and Hygiene*. 1993; 48(6):739–41. PMID: 8333566
29. Hommel M, Elliott SR, Soma V, Kelly G, Fowkes FJ, Chesson JM, et al. Evaluation of the antigenic diversity of placenta-binding *Plasmodium falciparum* variants and the antibody repertoire among pregnant women. *Infect Immun*. 2010; 78(5):1963–78. <https://doi.org/10.1128/IAI.01365-09> PMID: 20160014.
30. Chan JA, Howell KB, Langer C, Maier AG, Hasang W, Rogerson SJ, et al. A single point in protein trafficking by *Plasmodium falciparum* determines the expression of major antigens on the surface of infected erythrocytes targeted by human antibodies. *Cell Mol Life Sci*. 2016; 73(21):4141–58. <https://doi.org/10.1007/s00018-016-2267-1> PMID: 27193441.
31. Crabb BS, Cooke BM, Reeder JC, Waller RF, Caruana SR, Davern KM, et al. Targeted gene disruption shows that knobs enable malaria-infected red cells to cytoadhere under physiological shear stress. *Cell*. 1997; 89(2):287–96. PMID: 9108483
32. Deplaine G, Safeukui I, Jeddi F, Lacoste F, Brousse V, Perrot S, et al. The sensing of poorly deformable red blood cells by the human spleen can be mimicked in vitro. *Blood*. 2011; 117(8):e88–95. <https://doi.org/10.1182/blood-2010-10-312801> PMID: 21163923.
33. Kyes S, Pinches R, Newbold C. A simple RNA analysis method shows var and rif multigene family expression patterns in *Plasmodium falciparum*. *Mol Biochem Parasitol*. 2000; 105(2):311–5. PMID: 10693754.
34. Chappell LVL. Novel approaches for transcriptome analysis in Plasmodium parasites. Sanger Institute (Hinxton, Cambridge, England): 2014.
35. Kozarewa I, Ning Z, Quail MA, Sanders MJ, Berriman M, Turner DJ. Amplification-free Illumina sequencing-library preparation facilitates improved mapping and assembly of (G+C)-biased genomes. *Nat Methods*. 2009; 6(4):291–5. <https://doi.org/10.1038/nmeth.1311> PMID: 19287394.
36. Oyola SO, Otto TD, Gu Y, Maslen G, Manske M, Campino S, et al. Optimizing Illumina next-generation sequencing library preparation for extremely AT-biased genomes. *BMC Genomics*. 2012; 13:1. <https://doi.org/10.1186/1471-2164-13-1> PMID: 22214261.
37. Logan-Klumpler FJ, De Silva N, Boehme U, Rogers MB, Velarde G, McQuillan JA, et al. GeneDB—an annotation database for pathogens. *Nucleic Acids Res*. 2012; 40(Database issue):D98–108. <https://doi.org/10.1093/nar/gkr1032> PMID: 22116062.
38. Trapnell C, Pachter L, Salzberg SL. TopHat: discovering splice junctions with RNA-Seq. *Bioinformatics*. 2009; 25(9):1105–11. <https://doi.org/10.1093/bioinformatics/btp120> PMID: 19289445.
39. Anders S, Huber W. Differential expression analysis for sequence count data. *Genome Biol*. 2010; 11(10):R106. <https://doi.org/10.1186/gb-2010-11-10-r106> PMID: 20979621.
40. Rutherford K, Parkhill J, Crook J, Horsnell T, Rice P, Rajandream MA, et al. Artemis: sequence visualization and annotation. *Bioinformatics*. 2000; 16(10):944–5. PMID: 11120685.
41. Prieto JH, Koncarevic S, Park SK, Yates J 3rd, Becker K. Large-scale differential proteome analysis in *Plasmodium falciparum* under drug treatment. *PLoS One*. 2008; 3(12):e4098. <https://doi.org/10.1371/journal.pone.0004098> PMID: 19116658.
42. Jackson KE, Spielmann T, Hanssen E, Adisa A, Separovic F, Dixon MW, et al. Selective permeabilization of the host cell membrane of *Plasmodium falciparum*-infected red blood cells with streptolysin O and equinatoxin II. *Biochem J*. 2007; 403(1):167–75. <https://doi.org/10.1042/BJ20061725> PMID: 17155936.

43. Salanti A, Dahlback M, Turner L, Nielsen MA, Barfod L, Magistrado P, et al. Evidence for the involvement of VAR2CSA in pregnancy-associated malaria. *J Exp Med*. 2004; 200(9):1197–203. <https://doi.org/10.1084/jem.20041579> PMID: 15520249.
44. Bouyer G, Cueff A, Egee S, Kmiecik J, Maksimova Y, Glogowska E, et al. Erythrocyte peripheral type benzodiazepine receptor/voltage-dependent anion channels are upregulated by *Plasmodium falciparum*. *Blood*. 2011; 118(8):2305–12. <https://doi.org/10.1182/blood-2011-01-329300> PMID: 21795748.
45. Desai SA. Why do malaria parasites increase host erythrocyte permeability? *Trends in Parasitology*. 2014; 30(3):151–9. <http://dx.doi.org/10.1016/j.pt.2014.01.003>. PMID: 24507014
46. Nguiragool W, Bokhari AAB, Pillai AD, Rayavara K, Sharma P, Turpin B, et al. Malaria parasite clag genes determine nutrient uptake channel activity on infected red blood cells. *Cell*. 2011; 145(5):665–77. <https://doi.org/10.1016/j.cell.2011.05.002> PMID: 21620134
47. Berman PA, Human L, Freese JA. Xanthine oxidase inhibits growth of *Plasmodium falciparum* in human erythrocytes in vitro. *J Clin Invest*. 1991; 88(6):1848–55. <https://doi.org/10.1172/JCI115506> PMID: 1752946.
48. Martin RE, Kirk K. Transport of the essential nutrient isoleucine in human erythrocytes infected with the malaria parasite *Plasmodium falciparum*. *Blood*. 2007; 109(5):2217–24. <https://doi.org/10.1182/blood-2005-11-026963> PMID: 17047158.
49. Quashie NB, Dorin-Semlat D, Bray PG, Biagini GA, Doerig C, Ranford-Cartwright LC, et al. A comprehensive model of purine uptake by the malaria parasite *Plasmodium falciparum*: identification of four purine transport activities in intraerythrocytic parasites. *Biochem J*. 2008; 411(2):287–95. <https://doi.org/10.1042/BJ20071460> PMID: 18215139.
50. SA D. Insights Gained from *P. falciparum* Cultivation in Modified Media. *The Scientific World Journal*. 2013;363505. <https://doi.org/10.1155/2013/363505> PMID: 23956690
51. Hanssen E, Sougrat R, Frankland S, Deed S, Klonis N, Lippincott-Schwartz J, et al. Electron tomography of the Maurer's cleft organelles of *Plasmodium falciparum*-infected erythrocytes reveals novel structural features. *Mol Microbiol*. 2008; 67(4):703–18. <https://doi.org/10.1111/j.1365-2958.2007.06063.x> PMID: 18067543.
52. Chan JA, Howell KB, Reiling L, Ataide R, Mackintosh CL, Fowkes FJ, et al. Targets of antibodies against *Plasmodium falciparum*-infected erythrocytes in malaria immunity. *J Clin Invest*. 2012; 122(9):3227–38. <https://doi.org/10.1172/JCI62182> PMID: 22850879.
53. Cooke BM, Mohandas N, Coppel RL. The malaria-infected red blood cell: Structural and functional changes. *Advances in Parasitology*. Volume 50: Academic Press; 2001. p. 1–86.
54. Wickham ME, Rug M, Ralph SA, Klonis N, McFadden GI, Tilley L, et al. Trafficking and assembly of the cytoadherence complex in *Plasmodium falciparum*-infected human erythrocytes. *EMBO Journal*. 2001; 20(20):5636–49. <https://doi.org/10.1093/emboj/20.20.5636> PMID: 11598007
55. Cooke BM, Glenister FK, Mohandas N, Coppel RL. Assignment of functional roles to parasite proteins in malaria-infected red blood cells by competitive flow-based adhesion assay. *Br J Haematol*. 2002; 117(1):203–11. PMID: 11918556.
56. Duffy MF, Maier AG, Byrne TJ, Marty AJ, Elliott SR, O'Neill MT, et al. VAR2CSA is the principal ligand for chondroitin sulfate A in two allogeneic isolates of *Plasmodium falciparum*. *Mol Biochem Parasitol*. 2006; 148(2):117–24. <https://doi.org/10.1016/j.molbiopara.2006.03.006> PMID: 16631964.
57. Beeson JG, Rogerson SJ, Cooke BM, Reeder JC, Chai W, Lawson AM, et al. Adhesion of *Plasmodium falciparum*-infected erythrocytes to hyaluronic acid in placental malaria. *Nat Med*. 2000; 6(1):86–90. <https://doi.org/10.1038/71582> PMID: 10613830.
58. Cooke BM, Usami S, Perry I, Nash GB. A simplified method for culture of endothelial cells and analysis of adhesion of blood cells under conditions of flow. *Microvasc Res*. 1993; 45(1):33–45. <https://doi.org/10.1006/mvre.1993.1004> PMID: 8479340.
59. Maier AG, Rug M, O'Neill MT, Beeson JG, Marti M, Reeder J, et al. Skeleton-binding protein 1 functions at the parasitophorous vacuole membrane to traffic PfEMP1 to the *Plasmodium falciparum*-infected erythrocyte surface. *Blood*. 2007; 109(3):1289–97. <https://doi.org/10.1182/blood-2006-08-043364> PMID: 17023587.
60. Foth BJ, Zhang N, Chahal BK, Sze SK, Preiser PR, Bozdech Z. Quantitative time-course profiling of parasite and host cell proteins in the human malaria parasite *Plasmodium falciparum*. *Mol Cell Proteomics*. 2011; 10(8):M110 006411. <https://doi.org/10.1074/mcp.M110.006411> PMID: 21558492.
61. Rhiel M, Bittl V, Tribensky A, Charnaud SC, Strecker M, Muller S, et al. Trafficking of the exported *P. falciparum* chaperone PfHsp70x. *Sci Rep*. 2016; 6:36174. <https://doi.org/10.1038/srep36174> PMID: 27824087.

62. Akinyi S, Hayden T, Gamboa D, Torres K, Bendezu J, Abdallah JF, et al. Multiple genetic origins of histidine-rich protein 2 gene deletion in *Plasmodium falciparum* parasites from Peru. *Sci Rep*. 2013; 3:2797. <https://doi.org/10.1038/srep02797> PMID: 24077522.
63. Viebig NK, Gamain B, Scheidig C, Lepolard C, Przyborski J, Lanzer M, et al. A single member of the *Plasmodium falciparum* var multigene family determines cytoadhesion to the placental receptor chondroitin sulphate A. *EMBO Rep*. 2005; 6(8):775–81. <https://doi.org/10.1038/sj.embor.7400466> PMID: 16025132.
64. Zhang Y, Huang C, Kim S, Golkaram M, Dixon MWA, Tilley L, et al. Multiple stiffening effects of nanoscale knobs on human red blood cells infected with *Plasmodium falciparum* malaria parasite. *Proceedings of the National Academy of Sciences*. 2015; 112(19):6068–73. <https://doi.org/10.1073/pnas.1505584112> PMID: 25918423
65. Florens L, Liu X, Wang Y, Yang S, Schwartz O, Peglar M, et al. Proteomics approach reveals novel proteins on the surface of malaria-infected erythrocytes. *Mol Biochem Parasitol*. 2004; 135(1):1–11. PMID: 15287581.
66. Pachlatko E, Rusch S, Müller A, Hemphill A, Tilley L, Hanssen E, et al. MAHRP2, an exported protein of *Plasmodium falciparum*, is an essential component of Maurer's cleft tethers. *Molecular Microbiology*. 2010; 77(5):1136–52. <https://doi.org/10.1111/j.1365-2958.2010.07278.x> PMID: 20624222
67. Proellocks NI, Herrmann S, Buckingham DW, Hanssen E, Hodges EK, Elsworth B, et al. A lysine-rich membrane-associated PHISTb protein involved in alteration of the cytoadhesive properties of *Plasmodium falciparum*-infected red blood cells. *FASEB J*. 2014; 28(7):3103–13. <https://doi.org/10.1096/fj.14-250399> PMID: 24706359.
68. Oberli A, Slater LM, Cutts E, Brand F, Mundwiler-Pachlatko E, Rusch S, et al. A *Plasmodium falciparum* PHIST protein binds the virulence factor PfEMP1 and comigrates to knobs on the host cell surface. *FASEB J*. 2014; 28(10):4420–33. <https://doi.org/10.1096/fj.14-256057> PMID: 24983468.
69. Ward P, Equinet L, Packer J, Doerig C. Protein kinases of the human malaria parasite *Plasmodium falciparum*: the kinome of a divergent eukaryote. *BMC Genomics*. 2004; 5:79. <https://doi.org/10.1186/1471-2164-5-79> PMID: 15479470.
70. Schneider AG, Mercereau-Pujalon O. A new Apicomplexa-specific protein kinase family: multiple members in *Plasmodium falciparum*, all with an export signature. *BMC Genomics*. 2005; 6:30. <https://doi.org/10.1186/1471-2164-6-30> PMID: 15752424.
71. Nunes MC, Okada M, Scheidig-Benatar C, Cooke BM, Scherf A. *Plasmodium falciparum* FIKK Kinase Members Target Distinct Components of the Erythrocyte Membrane. *PLoS ONE*. 2010; 5(7):e11747. <https://doi.org/10.1371/journal.pone.0011747> PMID: 20668526
72. Kats LM, Fernandez KM, Glenister FK, Herrmann S, Buckingham DW, Siddiqui G, et al. An exported kinase (FIKK4.2) that mediates virulence-associated changes in *Plasmodium falciparum*-infected red blood cells. *Int J Parasitol*. 2014; 44(5):319–28. <https://doi.org/10.1016/j.ijpara.2014.01.003> PMID: 24530877.
73. Hatherley R, Blatch GL, Bishop OT. *Plasmodium falciparum* Hsp70-x: a heat shock protein at the host-parasite interface. *J Biomol Struct Dyn*. 2014; 32(11):1766–79. <https://doi.org/10.1080/07391102.2013.834849> PMID: 24028577.
74. Jha P, Laskar S, Dubey S, Bhattacharyya MK, Bhattacharyya S. *Plasmodium* Hsp40 and human Hsp70: A potential cochaperone-chaperone complex. *Mol Biochem Parasitol*. 2017; 214:10–3. <https://doi.org/10.1016/j.molbiopara.2017.03.003> PMID: 28322872.